# Mechanisms of self-similar pulses generation in a normal dispersion-decreasing fiber*

**FENG You-ceng**(冯又层)[1]** **and XIA Ge**(夏舸)[2]

*1. College of Electronics Information Engineering, South-central University for Nationalities, Wuhan 430074, China*

*2. College of Electronic and Electrical Engineering, Wuhan Textile University, Wuhan 430073, China*

(Received 19 August 2011)



Based on the principle of virtual equivalent gain, the evolution of self-similar pulses in a normal dispersion-decreasing fiber is investigated. The occurrence of wave breaking during the process under highly nonlinear conditions and the effect of its revealed four-wave mixing on the process are also analyzed. The results indicate that the pulse spectrum broadening in the initial stage is dominated by self-phase modulation while by four-wave mixing in the later stage. The more intense nonlinearity is, the faster the pulse evolution converges to the self-similarity synchronously in both the time domain and the spectrum domain.

**Document code:** A **Article ID:** 1673-1905(2012)01-0052-4

**DOI** 10.1007/s11801-012-1101-8

In 2000, it was first demonstrated by Ferman that the pulse with any initial condition propagating in a normal-dispersion fiber amplifier can eventually evolve into a self-similar parabolic pulse with perfect linear chirp[1]. The outstanding characteristic is very beneficial for applications, such as high-power pulse amplifying and pedestal-free pulse compression. Therefore it is of great significance for the performance improvement of ultra-high power short pulse lasers and ultra-high speed optical fiber communication system, and it is also has attracted a great deal of attention and intensive study in recent years[2-4].

In 2008, Fiont et al[5] showed that optical wave breaking (WB) still occurs during the process of pulse self-similar evolution in a normal-dispersion fiber amplifier under high nonlinear conditions, which manifests that four-wave mixing (FWM) takes effect too. In the present paper based on the principle of virtual equivalent gain, we extend the results to the normal dispersion-decreasing fiber, which has the typical hyperbic dispersion-decreasing distribution. Furthermore, we discuss the pulse self-similar evolution synchronously in both the time domain and the spectrum domain in detail, and focus on its corresponding mechanisms in the different evolving stages to reveal the important role, which FWM plays in the pulse spectral self-similar evolution.

The propagation of optical pulses in a normal dispersion-decreasing fiber can be described by a nonlinear Schrödinger (NLS) equation with varying group-velocity dispersion (GVD) coefficients[6]

$$\mathrm{i}\frac{\partial \boldsymbol{q}}{\partial z}-\frac{\beta_2}{2}D(z)\frac{\partial^2 \boldsymbol{q}}{\partial t^2}+\gamma\,|\,\boldsymbol{q}\,|^2\,\boldsymbol{q}=0\,, \tag{1}$$

where the $\boldsymbol{q}(z,t)$ is the complex amplitude of the slowly varying optical field, $z$ is the propagation distance in the fiber, $t$ is the time coordinate in a frame of reference that copropagates with the pulse, $\gamma$ is the nonlinearity coefficient, and $\beta_2$ is the GVD value at $z$=0 of the fiber. The normalized function $1\geqslant D(z)>0$ describes the variation of the fiber's GVD along its length. Define the new distance coordinate $\xi$ and field amplitude $\boldsymbol{u}(\xi, t)$ by variable substitution as

$$\xi=\int_0^z D(x)\mathrm{d}x\ , \tag{2}$$

$$\boldsymbol{u}(\xi,t)=\frac{\boldsymbol{q}(\xi,t)}{\sqrt{D(\xi)}}\ . \tag{3}$$

For a typical distribution of dispersion-decreasing hyperbolical profile

$$D(z)=\frac{1}{1+\Gamma_0 z}\ , \tag{4}$$

* This work has been supported by the School Key Fund of South-central University for Nationalities (No.yzz05008), and the Hubei Provincial Department of Education (No.Q20101613).

** E-mail: fengyc@mail.scuec.edu.cn

it is convenient to rewrite Eq.(1) as

$$\mathrm{i}\frac{\partial \boldsymbol{u}}{\partial \xi}-\frac{\beta_2}{2}\frac{\partial^2 \boldsymbol{u}}{\partial t^2}+\gamma|\boldsymbol{u}|^2\boldsymbol{u}=\mathrm{i}\frac{\Gamma_0}{2}\boldsymbol{u}\ . \tag{5}$$

Eq.(5) is in the form of the standard equation which describes the propagation of pulse in a fiber amplifier with normal dispersion. $\Gamma_0$ is the virtual constant gain since it does not exist really. It is worth noting that both Eq.(1) and its equivalent Eq.(5) can be used for describing the same pulse propagation in the fiber. The transformation between the real distance and its equivalent one is given by Eq.(2), while the amplitude transformation is given by Eq.(3). The pulse's equivalent duration keeps equal to its real value.

During seed pulse propagating in a normal dispersion fiber, the self-phase modulation (SPM)-induced frequency chirp is nonlinear while the dispersion-induced frequency chirp is linear, and the combined chirp remains nonlinear under high nonlinear conditions. It is well known that WB results from this nonlinear chirp. In the case of normal dispersion, the red- (blue-) shifted light near the leading (trailing) edge travels faster (slower) than the unshifted pulse parts. Once the shifted light overtakes the unshifted one, the pulse leading (trailing) regions contain light with different frequencies which interfere and generate new frequencies. The pulse spectral sidelobes and temporal fine oscillation structure are generated at the same time, and WB takes place. The phenomena can be viewed as results of FWM process[7], which are the same in the normal dispersion fiber amplifier as well. By introducing an effective length $\xi_{\mathrm{wbeff}}=(\exp(\xi_{\mathrm{wb}}\Gamma_0)-1)/\Gamma_0$, we can obtain the equivalent WB distance[5]

$$\xi_{\mathrm{wb}}\xi_{\mathrm{wbeff}}\approx\frac{\exp(3/2)}{4}L_{\mathrm{d}}L_{\mathrm{nl}}\ . \tag{6}$$

Substituting Eq.(4) into Eq.(2) yields the real WB distance as

$$z_{\mathrm{wb}}=(\exp(\xi_{\mathrm{wb}}\Gamma_0)-1)/\Gamma_0\ . \tag{7}$$

Thus the WB distance in the normal dispersion-decreasing fiber can be determined by Eqs.(6) and (7).

The above theoretical predictions are confirmed by numerical simulation. All the pulse and fiber parameters are chosen from Ref.[6]. A Gaussian chirp-free input pulse is with $T_{\mathrm{FWHM}}=1.0$ ps and pulse energy of 40 pJ, so the peak power of pulse is $P_0=37.6$ W. The fiber's parameters are $\gamma=3.33\ \mathrm{km^{-1}\,W^{-1}}$, $\beta_2=1.25\ \mathrm{ps^2/km}$, $\Gamma_0=0.028\ \mathrm{m^{-1}}$. The conditions correspond to dispersion length $L_{\mathrm{d}}=T_0^2/|\beta_2|=288$ m and nonlinearity length $L_{\mathrm{nl}}=1/(\gamma P_0)=8$ m, yielding the number of soliton as $N_0=(L_{\mathrm{d}}/L_{\mathrm{nl}})^{1/2}=6$. The real WB distance is calculated by Eqs.(6) and (7) as $z_{\mathrm{wb0}}\approx 0.236L_{\mathrm{d}}$.

The occurrence of WB can be judged by the oscillation appearing in the pulse edges[8]. However, compared with the pulse temporal profile, the pulse chirp is much more sensitive to the variations, because the chirp is proportional to the pulse intensity derivative of the time. So the distance, where WB happens, can also be determined by the chirp oscillations appearing in the pulse edges, which is a more precise determining method proposed in our previous work[9]. Fig.1 shows the pulse chirp evolution along the fiber at different lengths. From Fig.1, we can observe that the chirp oscillation in the pulse edges is very weak at $z=0.236L_{\mathrm{d}}$ since the WB just happens, and it becomes much more obvious at $z=0.260L_{\mathrm{d}}$ as the distance is increased a little. The numerical results agree well with the analytical results. With further pulse propagation at $z=0.300L_{\mathrm{d}}$, we can see clearly that the chirp oscillation region is expanded and oscillation amplitude is increased, indicating that WB becomes more severe and FWM is enhanced, thus allowing for the further pulse spectral broadening because of the new frequencies generated. As illustrated in Fig.2(b), the pulse spectral broadening is dominated gradually by the widening of pulse sidelobes after WB occurrence. This is quite different from the initial stage before WB occurrence, in which the spectral broadening is dominated by the expansion of ripples in the central part of pulse spectrum, which is the typical SPM-induced pulse spectral broadening. During the process, the ripples in the central part of pulse spectrum tend to be smooth, and the SPM effect nearly disappears. From these we can see that the WB limit point is the very threshold that FWM begins to take effect together with the SPM thereafter, and the dominant nonlinear mechanism for the pulse spectral broadening is being taken over from SPM to FWM gradually. These results are consistent with the conclusions which are drawn in the study of supercontinuum generation in normal dispersion-flattened fiber[9]. It is because of the energy being transferred from the center of spectrum to the wings by FWM, and the pulse spectral intensity in the center keeps on rising while the opposite case occurs in the wings, just as shown in

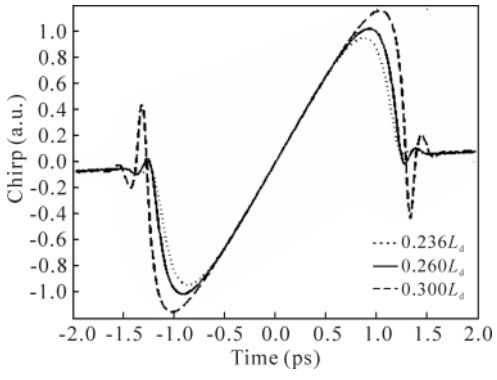


**Fig.1 Chirp evolution of pulse traveling through the fiber with different lengths**

Fig.2(b).

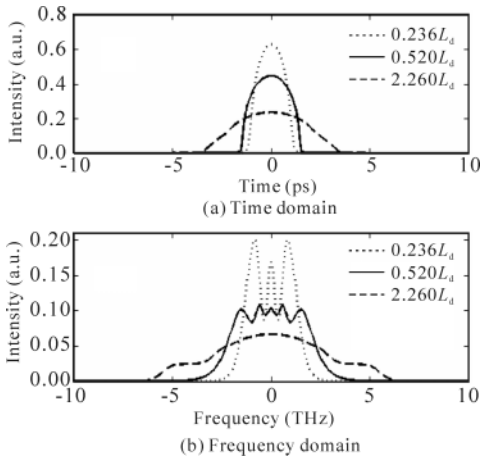


**Fig.2 Time and spectral profiles of the pulse during the evolution of self-similarity**

Comparing Fig.2(a) with Fig.2(b), we can see that the profile of the pulse spectral intensity changes much more severely than that of the pulse temporal intensity during the pulse self-similar evolution. The formation of self-similar pulse requires that the pulse evolution should converge synchronously in both the time domain and the spectrum domain[10]. To describe the pulse evolution quantitatively, two dimensionless functions $K$t and $K$s are introduced to characterize the pulse shape, which are defined as[11]

$$K\,\mathrm{t}[\boldsymbol{q}(z,t)]=\frac{\int_{-\infty}^{\infty}t^2\,|\,\boldsymbol{q}(z,t)\,|^2\,\mathrm{d}t\cdot\left(\int_{-\infty}^{\infty}|\,\boldsymbol{q}(z,t)\,|^4\,\mathrm{d}t\right)^2}{\left(\int_{-\infty}^{\infty}|\,\boldsymbol{q}(z,t)\,|^2\,\mathrm{d}t\right)^5}\quad,\qquad(8)$$

$$K\,\mathrm{s}[\boldsymbol{s}(z,\omega)]=\frac{\int_{-\infty}^{\infty}\omega^2\,|\,\boldsymbol{s}(z,\omega)\,|^2\,\mathrm{d}\omega\cdot\left(\int_{-\infty}^{\infty}|\,\boldsymbol{s}(z,\omega)\,|^4\,\mathrm{d}\omega\right)^2}{\left(\int_{-\infty}^{\infty}|\,\boldsymbol{s}(z,\omega)\,|^2\,\mathrm{d}\omega\right)^5}\quad,\qquad(9)$$

where $\boldsymbol{s}(z,\omega)$ is the Fourier transformation of $\boldsymbol{q}(z,t)$ in the time domain. The structural functional $K$t parameter is a function of slowly varying pulse envelope $\boldsymbol{q}(z,t)$, while $K$s parameter is a function of slowly varying pulse spectrum envelope $\boldsymbol{s}(z,\omega)$. Each pulse shape has its own characteristic factor. It is well known that $K$ = 0.0796 is for a Gaussian pulse and $K$ = 0.0720 is for an ideal parabolic pulse. The more $K$t and $K$s are close to 0.0720, the better the pulse evolves into a self-similar parabolic pulse.

We now consider the effect of nonlinearity on the pulse self-similar evolution. Fig.3 (Fig.4) shows the evolution of $K$t ($K$s) in a $5L_d$ (1440 m) transmission distance, which is long enough under different $N$ values conditions. For clear comparison, $N$ values are acquired by $N_0$ reduced (or increased) 2 times and 4 times. Comparing Fig.3 with Fig.4, we can see that the fluctuation range of $K$s curve is much larger than that of $K$t curve for the same $N$ value, which indicates that the pulse shape changes much more severely in the spectrum domain than in the time domain indeed during the self-similar evolution. In addition, both Fig.3 and Fig.4 show that in the initial stage, the larger $N$ value, the larger oscillation of pulse shape characteristic factor. But with shorter oscillation distance, it represents faster access to the steady self-similar evolution stage. Furthermore, we can observe from Figs.3 and 4 that the larger $N$ value is, the faster $K$t and $K$s curves converge synchronously, which indicates that the pulse can more quickly approach the self-similar evolution state. Thus it can be seen that the more intense nonlinearity is, the faster the pulse evolution converges to the self-similarity synchronously in both the time domain and the spectrum domain. It can be explained as follows: the more intense nonlinearity leads to the shorter WB distance (shown in Tab.1) as well as more severe WB. Thereby FWM acts more early and intensively. The dominant nonlinear mechanism for the pulse spectral broadening is more quickly taken over from SPM (in the initial stage) to FWM (in the later stage), and it results in the pulse spectral profile evolving more quickly from a ripple structure to a smooth near-parabolic profile.

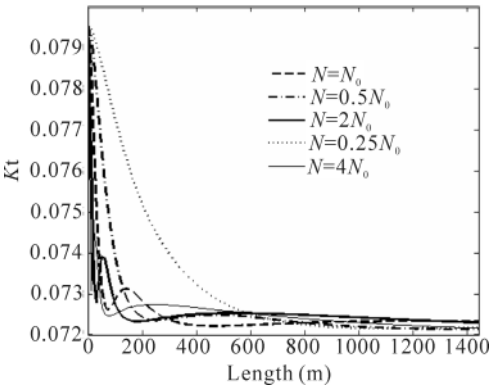


**Fig.3 Evolution curves of $K$t corresponding to different $N$ values along $5L_d$ transmission distance**

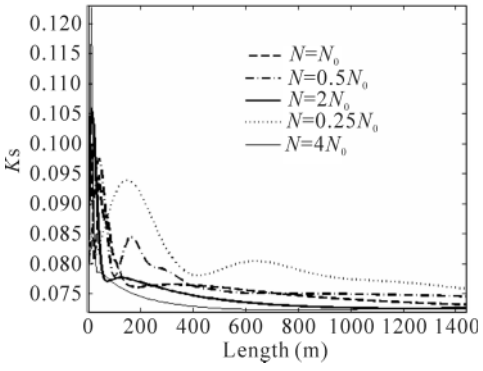


**Fig.4 Evolution curves of $K$s corresponding to different $N$ values along $5L_d$ transmission distance**

**Tab.1 WB distance vs. *N* value**

| $N/N_0$ | 0.25 | 0.5 | 1 | 2 | 4 |
|---|---|---|---|---|---|
| $z_{wb}/z_{wb0}$ | 6.88 | 2.57 | 1 | 0.46 | 0.21 |

The process of self-similar pulse generation in a normal dispersion-decreasing fiber is investigated. Furthermore the occurrence of WB and the effect of its revealed FWM on the process are also analyzed. Based on the principle of virtual equivalent gain, the equations used to determine WB distance are obtained and confirmed numerically by the pulse chirp oscillations. The results indicate that the pulse spectrum broadening in the initial stage is dominated by SPM while by FWM in the later stage. The more intense nonlinearity is, the faster the pulse evolution converges to the self-similarity synchronously in both the time domain and the spectrum domain.

## References

[1] Fermann M E, Kruglov V I, Thomsen B C, Dudley J M and Harvey J D, Physics Review Letters **84**, 6010 (2000).

[2] Dudley J M, Finot C, Richardson D J and Millot G, Nature Physics **3**, 597 (2007).

[3] Renninger W H, Chong A and Wise F W, Physics Review A **82**, 021805(R) (2010).

[4] Haghgoo S and Ponomarenko S A, Optics Express **19**, 9750 (2011).

[5] Finot C, Kibler B, Provost L and Wabnitz S, Journal of the Optical Society of America B **25**, 1938 (2008).

[6] Hirooka T and Nakazawa M, Optics Letters **29**, 498 (2004).

[7] Agrawal G P, Nonlinear Fiber Optics & Applications of Nonlinear Fiber Optics, Beijing: Electronics Industry Press, 71 (2010). (in Chinese)

[8] Anderson D, Desaix M, Lisak M and Quiroga M L, Journal of the Optical Society of America B **9**, 1358 (1992).

[9] XIA Ge, HUANG De-xiu and YUAN Xiu-hua, Acta Physics Sinica **56**, 2212 (2007). (in Chinese)

[10] Kruglov V I, Peacock A C, Harvey J D and Dudley J M, Journal of the Optical Society of America B **19**, 461 (2002).

[11] Lei T, Lu F, Tu C, Deng Y and Li E, Optics Express **17**, 585 (2009).